21. PALEOMAGNETISM OF SOME LEG 33 SEDIMENTS AND BASALTS

Robert S. Cockerham and Richard D. Jarrard,
Department of Geological Sciences, University of California, Santa Barbara

ABSTRACT

Stable remanent magnetizations were found in dominantly Cretaceous sediments from Holes 315A and 317A and in basalts from Hole 317A. Except for uppermost Cretaceous and Paleocene sediments from Hole 315A, virtually all samples were of normal polarity. Highly consistent inclinations of magnetization from the sediments at each site indicate about 15° of northward motion for each site since the Late Cretaceous. However, inclinations from 317A basalts are consistently about 20° steeper than inclinations of the overlying sediments.

INTRODUCTION

Paleomagnetic measurements were carried out on cores of both basalt and sediment from Holes 315A (Line Islands—4°10.26′N, 158°31.52′W) and 317A (Manihiki Plateau—11°00.09′S, 162°15.78′W). The objectives were to (1) determine the amount of northward motion for this area of the Pacific plate, and (2) investigate the Cretaceous reversal sequence.

METHODS AND DATA

Sediments

Eighty-four samples, upper Paleocene to Santonian in age, were taken from Hole 315A cores, and 33 samples of lower Maestrichtian-upper Campanian to Barremian-Aptian age were taken from Hole 317A cores (Figure 1). The 5.8-cc rectangular samples were cut with a diamond saw. All measurements of remanent magnetization were made on a 5-Hz Schonstedt SSM-1a spinner magnetometer. All samples were magnetically "cleaned" using a Schonstedt GSD-1 demagnetizer.

Ten samples (five from each site) were selected for step-wise AF demagnetization in fields of from 25 oe up to 400 oe (Table 1). In order to determine the optimum demagnetizing field for removal of most or all viscous magnetization, we calculated paleomagnetic stability indexes (PSI; Symons and Stupavsky, 1974). The PSI is an indication of the rate of change in direction of magnetization with demagnetization. A plot of the log of PSI against field strength (Figure 2) showed that a 100-oe field appeared to give minimum change of sample directions; therefore, all other samples were cleaned in this field. Curves of change in intensity of magnetization with increasing demagnetizing field generally show (Figure 3) a slow decrease in intensity beyond a 100-oe field, consistent with the conclusion that most viscous magnetization has been removed and that the remaining magnetization resides mainly in domains of relatively high coercive force.

Table 2 shows the directions of remanent magnetization and intensities of the samples after 100-oe AF demagnetization. Inclinations (Incl) are given with respect to the present horizontal, positive downward, assuming vertical drill cores. Negative inclinations indicate normal polarity, assuming a Southern Hemisphere origin. Declinations (Decl) are only relative to the split core face; because the cores are unoriented as to azimuth, the original declinations are indeterminate. *MM* and *A* are measures of the consistency of replicate measurements of intensity and direction of magnetization, respectively, on a single sample (Doell and Cox, 1965). Values of *MM* greater than 20% generally result from inhomogeneity of sample mangetization or from magnetization intensity near the noise level of the magnetometer. Values of *A* greater than 5° indicate that the direction of magnetization is poorly defined, generally because magnetization intensity is near the noise level of the magnetometer or because of instability of sample magnetization. Column F indicates age of the samples (see Part I, this volume).

Basalts

Twenty-four basalt samples, approximately 2.5 cm in diameter and 2.5 to 10 cm in length, were cored from the Manihiki Plateau (Hole 317A) basalt cores. Up to three specimens were cut from some samples for statistical purposes. The samples were cored either parallel or normal to the core axis. Paleomagnetic measurements were made either on the 5-Hz Schonstedt SSM1-a spinner magnetometer or a 120-Hz spinner magnetometer (Doell and Cox, 1965). All specimens were magnetically "cleaned" using a Schonstedt GSD-1 demagnetizer.

Eight specimens were selected for step-wise AF demagnetization in fields of 25 oe to 950 oe (Table 3). PSI values were calculated and log of PSI plotted against field strength (Figure 4) showed that a 200-250 oe field appeared to give minimum change of sample direction. The variation of intensity of magnetization upon demagnetization (Figure 5) was not a sensitive indicator of optimum demagnetizing field. In general, PSI values at 250 oe were less than 50 millioersted/degree, which is indicative of very stable samples (Symons and Stupavsky, 1974). Several specimens were stored in

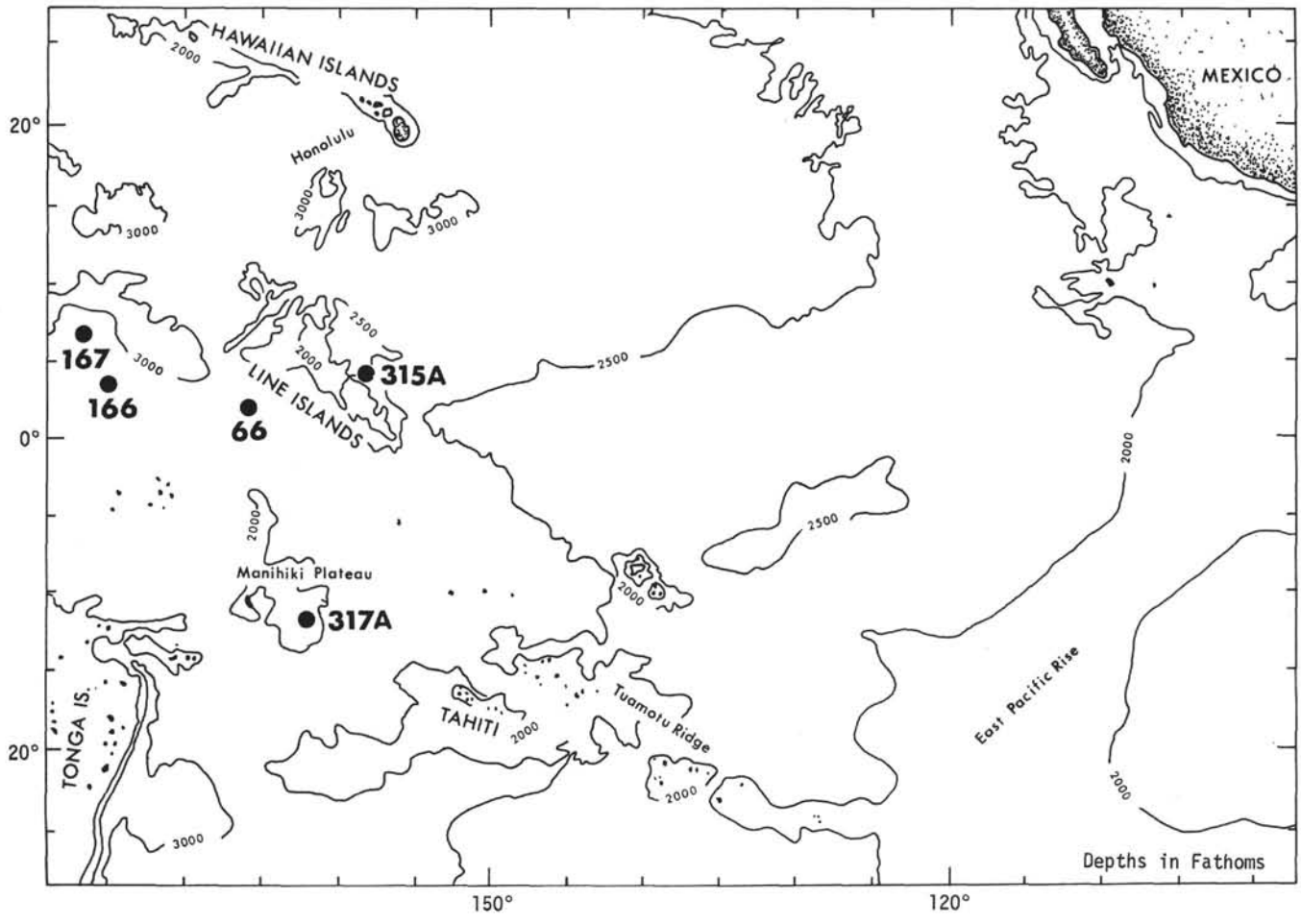

Figure 1. *Location of DSDP Sites 66, 166, 167, and Holes 315A and 317A.*

wooden cabinets in the earth's field for 2 months and then remeasured. The direction change was ±4° for inclination and ±7° for declination. When demagnetized at the previous peak field, the directions varied by only a few tenths of a degree from the initial measurements. The peak alternating fields required to reduce the remanence to 50% of its initial value (median destructive field—MDF) were between 200 and 320 oe. These MDF values are comparable to values obtained from most other DSDP basalts (Lowrie et al., 1973a, b) and for dredged basalts from the mid-Atlantic ridge (Park and Irving, 1970). However, Marshall (in preparation) presents data from North Pacific DSDP basalts which have a geometric mean MDF of only 90 oe.

Table 4 shows the directions of natural remanent magnetization (NRM) and directions after 200 or 250 oe AF demagnetization in addition to corresponding intensity, A, and MM values. Intensities of NRM range from 8.4×10^{-3} emu/cc to 1.9×10^{-3} emu/cc with a geometric mean of 4.3×10^{-3} emu/cc. These values are comparable to those reported for other DSDP basalts (Lowrie et al., 1973a, b; Marshall, in preparation; Peirce et al., 1974).

All of the basalt samples from Hole 317A have negative inclinations, indicating normal polarity. In order to check that no undetected reversely polarized flows exist between the sampled intervals, NRM polarity determinations were made on uncut basalt cylinders. A portable fluxgate magnetometer was used, with the fluxgate head within a mu-metal shield. The polarity of every cylindrical piece of basalt from Holes 315A (Cores 31 to 34) and 317A (Cores 31 to 34) was quickly and easily determined in this manner. The few small pieces of irregular shape were not measured because, unlike the cylindrical pieces, their original orientation with respect to the vertical could not be determined. Virtually all pieces from both sites had negative inclinations and thus normal polarity. The only exceptions were six very short pieces (≤2 cm) from Hole 317A which, based on their shape, appeared to have been inverted by the drilling process. Apparently about one-fourth of the pieces 1-2 cm in length were inverted during drilling and coring. A fluxgate magnetometer appears to be an efficient and accurate method of determining the original orientation of these small basalt pieces.

The polarity determinations on basalt pieces were of the NRM only; the pieces were not demagnetized. Because the demagnetization of individual specimens from the Hole 317A basalts (Table 3) indicates high stability of magnetization, the NRM polarities are probably reliable indicators of original thermal remanent magnetization (TRM) polarities. Demagnetization of pilot specimens from Hole 315A basalts has just begun; preliminary measurements indicate much lower

TABLE 1
Demagnetization of Hole 315A and 317A Sediment Pilot Samples

Sample (Interval in cm)	Demagnetization Field	Incl. (degrees)	Decl. (degrees)	*A* (degrees)	Intensity emu/cc	*MM* (%)
315A-15-2, 38	000	23.1	107.9	0.2	$4.41E^{-5}$	7.3
	025	16.2	105.9	0.1	$3.93E^{-5}$	5.5
	050	18.1	105.9	0.3	$1.50E^{-5}$	8.0
	075	27.5	105.5	0.1	$4.72E^{-6}$	11.4
	100	63.6	106.3	3.9	$1.56E^{-6}$	11.5
	150	16.7	348.0	0.7	$1.46E^{-6}$	10.5
	200	1.9	32.7	0.9	$2.33E^{-6}$	6.2
	250	-2.7	57.1	0.8	$4.24E^{-6}$	6.3
	300	-1.6	62.5	3.8	$6.85E^{-6}$	6.2
	400	-4.7	72.5	1.8	$9.91E^{-6}$	4.3
315A-16-2, 80	000	24.4	287.7	0.5	$3.25E^{-5}$	7.0
	025	27.1	304.9	0.7	$3.10E^{-5}$	7.2
	050	17.9	314.6	0.4	$3.85E^{-5}$	6.9
	075	15.0	316.9	0.6	$4.08E^{-5}$	5.9
	100	13.7	318.3	0.8	$3.96E^{-5}$	5.7
	150	12.7	322.9	0.4	$3.47E^{-5}$	7.9
	200	11.6	328.1	0.8	$2.70E^{-5}$	5.2
	250	10.2	338.5	0.7	$2.10E^{-5}$	5.9
	300	9.2	355.3	0.2	$1.67E^{-5}$	5.2
	350	6.9	16.4	0.4	$1.45E^{-5}$	6.1
	400	5.4	35.9	0.3	$1.48E^{-5}$	4.7
315A-20-2, 8	000	-15.0	63.6	1.0	$1.88E^{-5}$	9.9
	025	-13.8	63.3	1.0	$1.83E^{-5}$	9.4
	050	-13.5	64.1	0.7	$1.81E^{-5}$	9.7
	075	-13.0	63.5	0.8	$1.78E^{-5}$	8.6
	100	-13.5	64.4	0.9	$1.70E^{-5}$	8.9
	150	-13.6	64.1	0.7	$1.59E^{-5}$	9.1
	200	-13.6	64.2	0.9	$1.45E^{-5}$	9.7
	250	-16.5	65.6	1.5	$1.36E^{-5}$	9.0
	300	-12.7	62.9	1.2	$1.55E^{-5}$	29.1
	400	-13.5	64.7	0.8	$1.10E^{-5}$	9.9
315A-25-2, 134	000	-23.3	304.6	0.6	$5.24E^{-5}$	18.5
	025	-22.0	304.2	0.5	$4.93E^{-5}$	18.7
	050	-20.3	304.4	0.5	$4.32E^{-5}$	19.3
	075	-18.8	306.6	0.1	$4.00E^{-5}$	22.4
	100	-18.1	304.8	0.3	$3.52E^{-5}$	20.0
	150	-19.2	305.4	1.7	$2.77E^{-5}$	21.5
	200	-16.3	306.9	0.8	$2.26E^{-5}$	22.0
	250	-16.1	322.0	1.7	$2.04E^{-5}$	18.5
	300	-18.3	314.5	0.1	$1.34E^{-5}$	23.8
	400	-21.5	327.5	0.4	$8.06E^{-6}$	25.2
315A-26-1, 45	000	-47.7	236.6	1.2	$5.42E^{-5}$	7.7
	025	-44.3	235.4	0.6	$3.58E^{-5}$	7.5
	050	-46.1	231.7	0.2	$1.77E^{-5}$	7.9
	075	-49.7	224.1	1.7	$1.08E^{-5}$	9.0
	100	-53.9	242.6	0.1	$7.54E^{-6}$	10.9
	150	-59.7	170.6	0.2	$4.69E^{-6}$	7.3
	200	-58.6	66.4	1.7	$3.69E^{-6}$	11.4
	250	-33.9	67.9	0.2	$4.61E^{-6}$	7.5
	300	-34.1	62.0	0.3	$5.24E^{-6}$	6.2
	350	-26.5	60.2	0.0	$5.44E^{-6}$	7.4
	400	-19.6	64.4	0.3	$6.00E^{-6}$	6.0
317A-5-1, 134	000	-18.0	126.6	0.7	$1.00E^{-5}$	6.9
	025	-15.2	125.4	0.2	$1.27E^{-5}$	5.0
	050	-9.6	118.5	0.3	$5.38E^{-6}$	2.6
	075	0.9	100.6	0.4	$1.94E^{-6}$	7.6

TABLE 1 – *Continued*

Sample (Interval in cm)	Demagnetization Field	Incl. (degrees)	Decl. (degrees)	*A* (degrees)	Intensity emu/cc	*MM* (%)
	100	22.4	60.6	0.4	$1.08E^{-6}$	15.2
	150	37.3	23.6	4.7	$1.36E^{-6}$	27.1
	200	20.3	31.7	0.1	$1.92E^{-6}$	12.0
	250	12.9	44.0	0.4	$2.32E^{-6}$	9.2
	300	5.9	58.6	0.3	$2.84E^{-6}$	7.6
	400	2.0	71.0	0.2	$3.98E^{-6}$	5.5
	000	-34.9	186.9	1.7	$5.23E^{-5}$	9.4
317A-7-1, 144	025	-30.3	171.2	1.0	$4.75E^{-5}$	7.1
	050	-30.8	163.8	1.2	$3.14E^{-5}$	6.3
	075	-31.0	159.1	1.1	$2.38E^{-5}$	4.1
	100	-31.1	156.9	2.0	$2.16E^{-5}$	12.8
	125	-25.3	155.3	1.2	$1.93E^{-5}$	4.8
	150	-23.2	153.3	1.4	$1.78E^{-5}$	6.1
	175	-31.6	137.6	1.7	$1.42E^{-5}$	3.6
	200	-30.2	129.4	1.6	$1.30E^{-5}$	4.5
	250	-26.8	115.2	0.9	$1.19E^{-5}$	4.6
	300	-7.4	132.0	1.2	$1.39E^{-5}$	5.7
	400	-12.9	93.5	0.0	$1.29E^{-5}$	5.2
317A-11-2, 67	000	-41.3	230.3	0.5	$5.11E^{-5}$	5.3
	025	-41.1	227.7	0.4	$4.86E^{-5}$	5.5
	050	-43.3	225.2	0.4	$4.26E^{-5}$	5.3
	075	-44.8	224.7	0.5	$3.75E^{-5}$	5.3
	100	-45.5	224.8	0.1	$3.36E^{-5}$	5.2
	150	-47.3	227.1	1.6	$2.64E^{-5}$	8.5
	200	-49.2	223.1	0.1	$1.94E^{-5}$	4.8
	250	-52.9	221.3	0.9	$1.38E^{-5}$	4.4
	300	-58.1	216.9	0.0	$9.69E^{-6}$	4.1
	400	-74.2	159.6	0.1	$4.86E^{-6}$	3.7
317A-13-3, 67	000	-57.9	348.1	0.8	$5.42E^{-5}$	9.1
	025	-58.8	349.0	0.8	$5.36E^{-5}$	9.3
	050	-59.8	349.9	0.9	$5.21E^{-5}$	9.0
	075	-59.9	350.0	0.7	$4.96E^{-5}$	8.8
	100	-59.9	350.0	0.9	$4.75E^{-5}$	9.2
	150	-59.8	350.5	0.9	$4.24E^{-5}$	8.7
	200	-60.3	350.7	1.1	$3.66E^{-5}$	9.0
	250	-60.4	352.1	1.1	$3.10E^{-5}$	9.3
	300	-61.0	352.7	1.1	$2.57E^{-5}$	9.1
	400	-59.0	357.7	1.3	$1.64E^{-5}$	9.5
317A-13-3, 144	000	-61.3	192.7	0.0	$1.69E^{-4}$	5.0
	025	-60.8	191.1	0.3	$1.68E^{-4}$	5.1
	050	-60.8	189.6	0.1	$1.66E^{-4}$	4.4
	075	-60.5	188.2	0.3	$1.64E^{-4}$	5.3
	100	-60.5	187.7	0.1	$1.58E^{-4}$	4.5
	150	-61.4	184.5	0.3	$1.41E^{-4}$	4.9
	200	-62.0	183.1	0.4	$1.15E^{-4}$	4.7
	250	-62.9	181.3	0.6	$9.07E^{-5}$	4.9
	300	-64.7	176.0	0.3	$6.99E^{-5}$	5.3
	400	-66.0	157.3	0.9	$4.17E^{-5}$	5.5

Note: See text for definitions of *A* and *MM*.

stability for these basalts. Thus it is possible that some of the negative inclinations determined for 315A basalts may result from a large component of viscous magnetization rather than the original TRM polarity. Acquisition of a viscous component in situ during the Brunhes normal polarity epoch could not account for the negative inclinations, since the site is now just north of the equator.

PALEOLATITUDES

Inclinations of remanent magnetization in Deep-Sea Drilling cores and piston cores provide a measure of

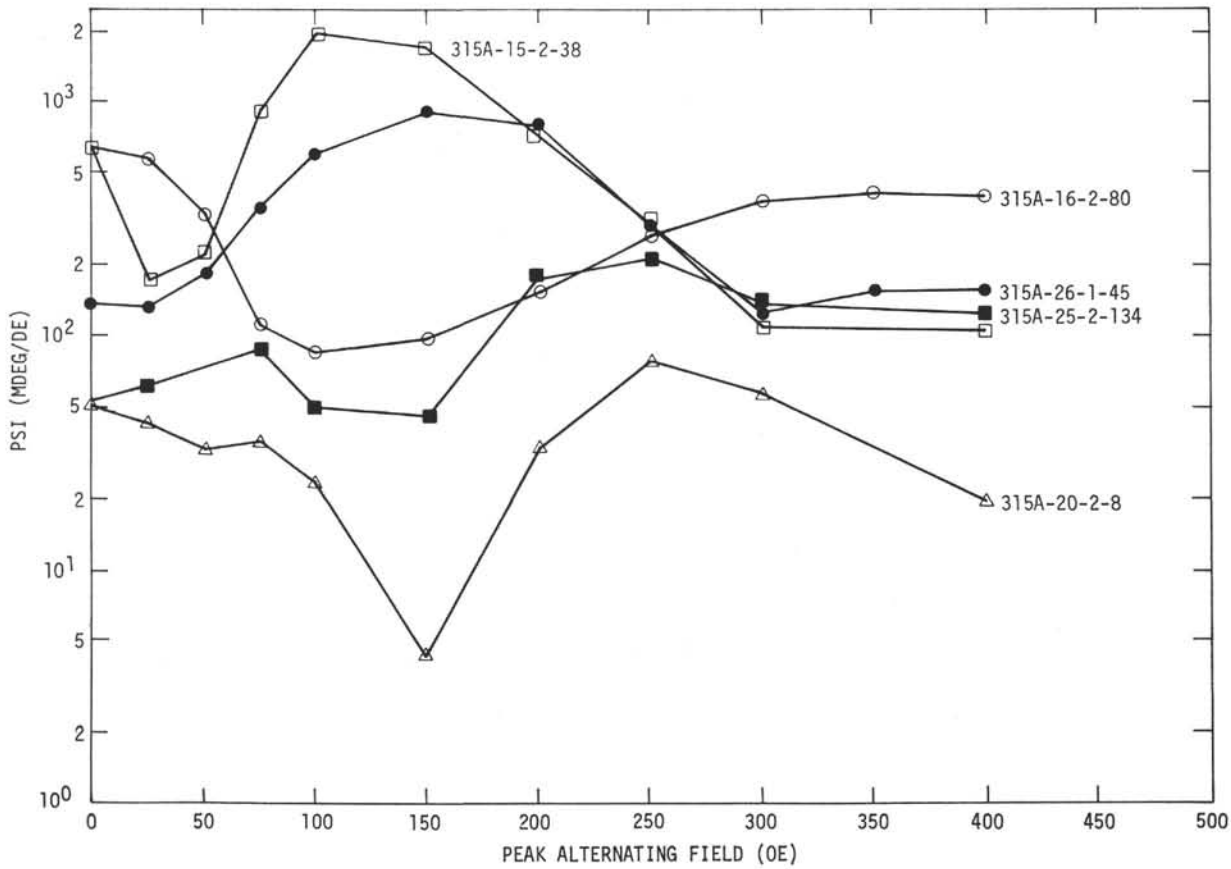

Figure 2a. *Log PSI demagnetization curves for DSDP Hole 315A sediment specimens. See text for discussion of PSI.*

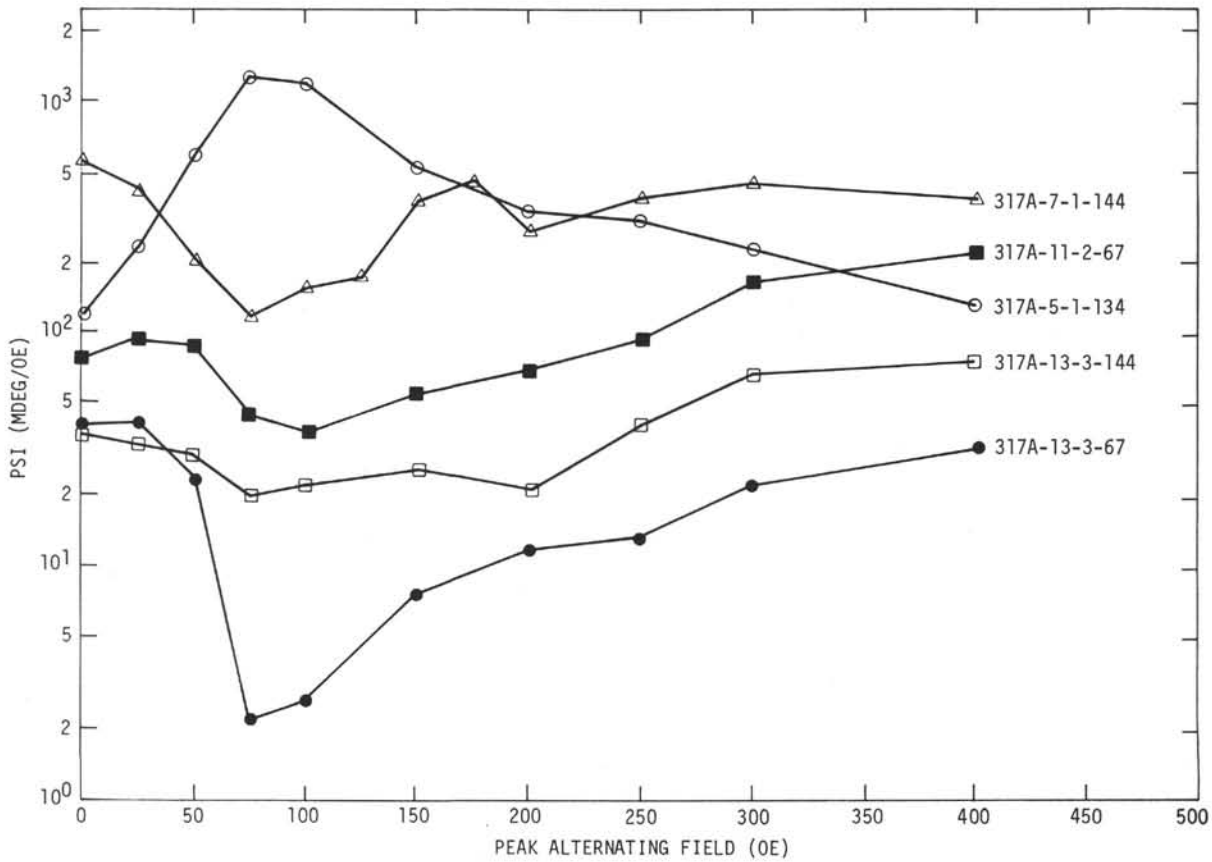

Figure 2b. *Log PSI demagnetization curves for DSDP Hole 317A sediment specimens. See text for discussion of PSI.*

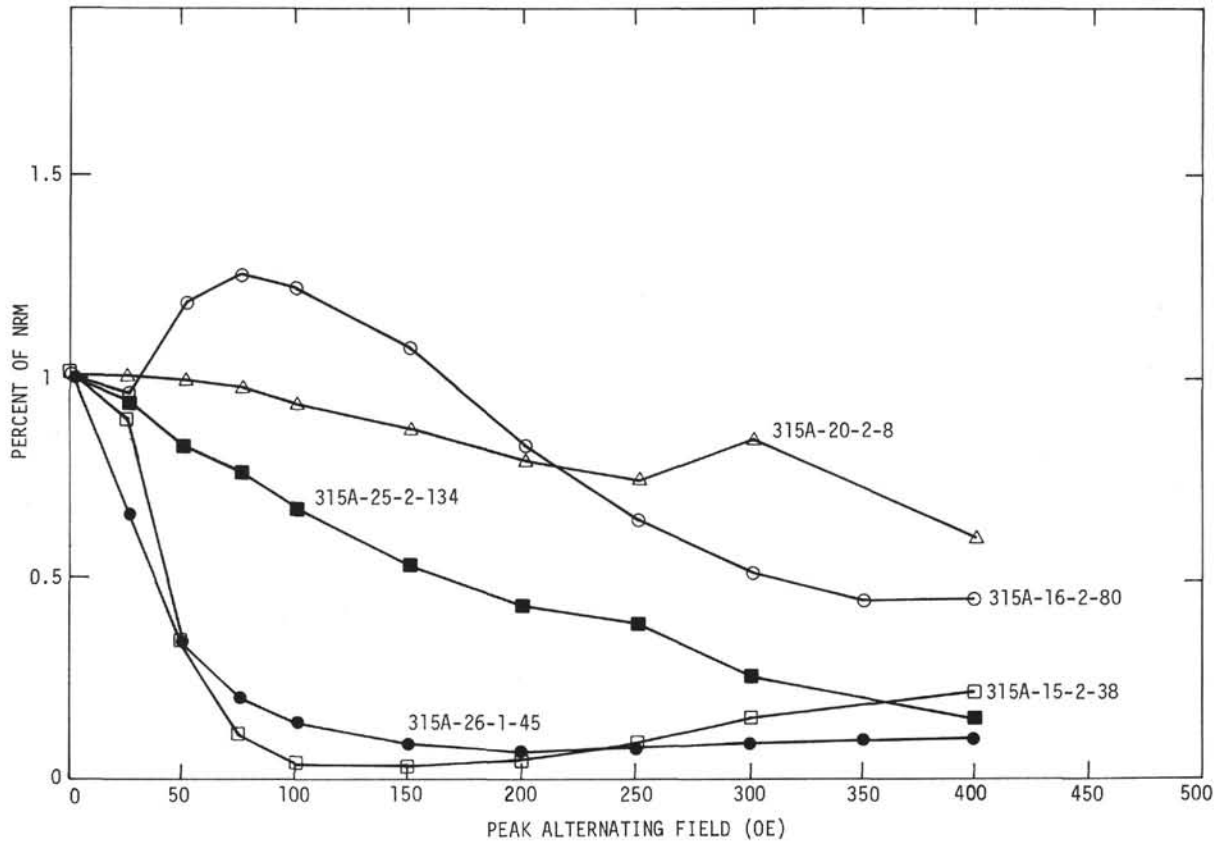

Figure 3a. *Progressive AF demagnetization curves for DSDP Hole 315A sediment specimens. Intensities are relative to the untreated (NRM) values.*

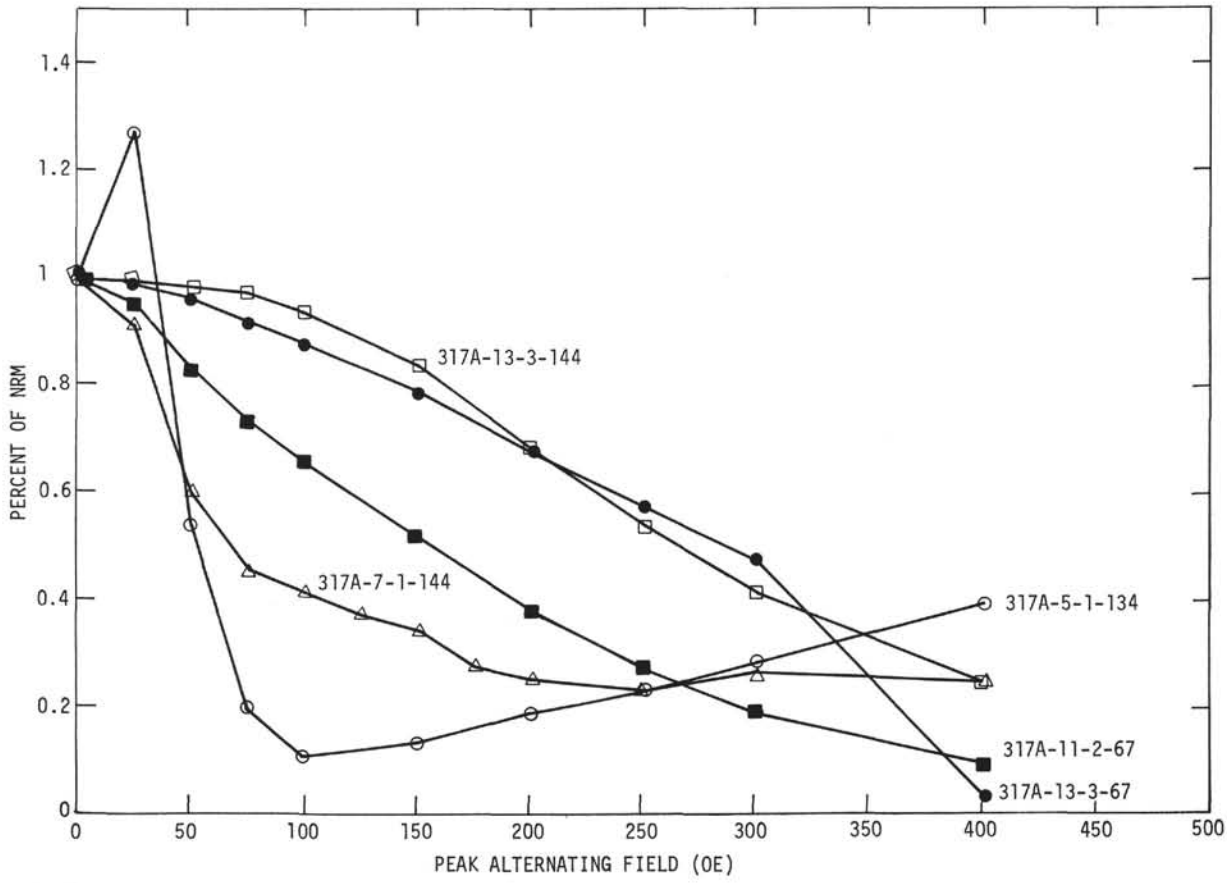

Figure 3b. *Progressive AF demagnetization curves for DSDP Hole 317A sediment specimens. Intensities are relative to the untreated (NRM) values.*

TABLE 2
Results of Paleomagnetic Measurements of Hole 315A and 317A Sediments

Sample (Interval in cm)	Demagnetization Field	Incl. (degrees)	Decl. (degrees)	*A* (degrees)	Intensity (emu/cc)	*MM* (%)	F (Age)
Hole 315A							
15-1, 82	100	28.9	305.6	1.4	$1.10E^{-6}$	6.5	
15-1, 84	100	25.7	315.4	0.6	$1.93E^{-6}$	5.8	Upper Paleocene
15-2, 38	100	63.6	106.3	3.9	$1.56E^{-6}$	11.5	
16-1, 133	100	9.3	204.0	0.7	$2.13E^{-5}$	10.5	
16-2, 54	100	-19.0	38.6	3.1	$1.59E^{-6}$	3.4	
16-2, 56	100	-17.6	50.0	0.9	$1.36E^{-6}$	10.8	
16-2, 58	100	-6.8	29.9	1.4	$9.73E^{-7}$	14.0	
16-2, 80	100	13.7	318.3	0.8	$3.96E^{-5}$	5.7	
16-2, 103	100	11.9	164.2	0.7	$5.29E^{-5}$	7.1	
16-2, 105	100	11.4	161.3	0.1	$5.13E^{-5}$	8.5	
17-1, 111	100	21.6	117.8	17.6	$2.24E^{-5}$	18.4	
17-2, 122	100	-12.4	147.1	0.3	$4.66E^{-6}$	15.5	
18-1, 122	100	14.6	305.9	0.5	$1.76E^{-5}$	11.7	
18-1, 124	100	18.6	307.1	3.6	$1.86E^{-5}$	11.2	
18-1, 126	100	20.7	321.2	0.1	$1.14E^{-6}$	16.2	
18-2, 121	100	18.8	296.1	0.8	$1.69E^{-5}$	9.2	
18-2, 123	100	29.7	297.6	1.6	$2.09E^{-5}$	5.5	
18-3, 122	100	20.7	1.2	1.6	$1.41E^{-6}$	10.6	Middle Maestrichtian
18-3, 124	100	23.7	353.3	1.3	$1.55E^{-6}$	10.0	
18-3, 126	100	48.5	337.1	31.9	$2.17E^{-6}$	35.6	
18-4, 83	100	-22.4	316.4	17.6	$2.20E^{-5}$	19.0	
18-4, 85	100	19.6	295.3	0.0	$1.40E^{-5}$	10.7	
19-1, 104	100	42.8	269.2	1.8	$2.63E^{-6}$	27.0	
19-1, 106	100	-25.5	283.0	0.5	$3.07E^{-6}$	15.2	
19-2, 107	100	-15.2	65.8	0.1	$3.31E^{-5}$	8.0	
19-3, 17	100	25.9	239.8	4.6	$2.38E^{-5}$	16.3	
19-3, 110	100	-16.9	57.7	0.4	$8.04E^{-6}$	4.7	
19-3, 112	100	-8.8	47.6	0.8	$1.17E^{-5}$	13.2	
19-4, 138	100	-17.2	147.5	0.1	$1.27E^{-5}$	4.7	
19-4, 140	100	-13.4	144.8	0.3	$1.47E^{-5}$	2.5	
19-5, 13	100	-16.9	288.2	0.1	$1.76E^{-5}$	6.4	
19-5, 70	100	-11.0	7.1	1.7	$2.24E^{-5}$	16.6	
19-5, 72	100	-15.3	4.3	0.1	$1.05E^{-5}$	13.9	
19-6, 5	100	14.8	172.2	0.4	$1.72E^{-5}$	11.6	
19-6, 44	100	-12.9	299.0	0.7	$1.96E^{-5}$	5.2	
19-6, 131	100	19.2	39.2	0.4	$1.25E^{-5}$	10.3	
20-2, 8	100	-13.5	64.4	0.9	$1.70E^{-5}$	8.9	
20-2, 90	100	-17.2	40.7	0.8	$2.74E^{-5}$	8.3	
20-2, 92	100	-12.3	47.1	0.2	$3.31E^{-5}$	4.4	
20-3, 8	100	-8.6	240.5	0.7	$5.85E^{-5}$	5.6	
20-3, 79	100	-16.3	131.1	0.4	$1.68E^{-5}$	8.4	
20-3, 148	100	-19.6	339.1	0.0	$4.41E^{-5}$	4.0	
20-4, 22	100	-19.4	226.0	0.3	$2.93E^{-5}$	3.6	
20-4, 95	100	-23.9	78.3	1.1	$8.93E^{-6}$	7.6	
20-5, 19	100	-23.4	77.9	0.7	$8.73E^{-6}$	9.4	
20-5, 128	100	-17.3	4.4	0.5	$3.03E^{-5}$	18.2	
20-5, 130	100	-18.9	356.5	0.4	$2.20E^{-5}$	5.6	Lower Maestrichtian-
21-1, 93	100	-22.8	213.0	5.2	$1.25E^{-4}$	14.9	upper Campanian
21-1, 95	100	-12.2	212.6	0.4	$1.17E^{-4}$	11.1	
21-2, 3	100	-9.9	170.3	0.2	$6.27E^{-5}$	3.4	
21-2, 5	100	-12.1	168.6	0.6	$4.27E^{-5}$	8.7	
21-2, 7	100	-17.6	172.7	0.0	$5.21E^{-5}$	4.0	
21-2, 70	100	8.7	183.5	0.0	$6.56E^{-5}$	4.2	
21-2, 72	100	13.8	174.5	0.1	$4.01E^{-5}$	7.0	
21-3, 22	100	-15.3	29.4	0.7	$1.15E^{-5}$	14.7	

TABLE 2 – *Continued*

Sample (Interval in cm)	Demagnetization Field	Incl. (degrees)	Decl. (degrees)	*A* (degrees)	Intensity $\frac{\text{emu}}{\text{cc}}$	*MM* (%)	F (Age)
21-3, 107	100	-32.5	140.1	0.3	$9.26E^{-6}$	4.3	Middle Maestrichtian
21-4, 11	100	-22.3	326.6	0.5	$1.30E^{-5}$	7.2	
21-4, 97	100	-9.7	276.6	0.9	$1.45E^{-5}$	16.1	
21-4, 140	100	-21.0	78.2	0.3	$7.63E^{-6}$	7.7	
21-5, 10	100	-22.5	23.3	0.2	$1.49E^{-5}$	6.3	
21-5, 114	100	-17.9	178.2	1.1	$1.53E^{-5}$	9.4	
21-5, 116	100	-17.6	179.4	0.4	$1.45E^{-5}$	4.3	
21-5, 118	100	-20.6	182.8	0.4	$1.36E^{-5}$	8.2	
21-6, 50	100	-9.7	250.3	0.2	$1.78E^{-5}$	5.7	
21-6, 103	100	-7.2	215.6	0.0	$4.63E^{-5}$	6.4	
21-6, 105	100	-13.0	222.6	1.1	$5.69E^{-5}$	4.4	
22-2, 11	100	-20.0	92.1	0.5	$1.51E^{-5}$	8.6	Middle Campanian
22-2, 138	100	-47.8	204.8	1.4	$7.66E^{-6}$	19.4	
22-2, 140	100	-30.6	228.2	0.7	$6.59E^{-6}$	5.9	
22-3, 24	100	-13.3	135.6	0.5	$1.94E^{-5}$	2.3	
22-3, 91	100	-6.3	210.1	0.5	$3.88E^{-5}$	9.6	
22-4, 26	100	-18.8	128.7	0.3	$4.34E^{-5}$	10.5	
25-2, 134	100	-18.1	304.8	0.3	$3.52E^{-5}$	20.0	Lower Campanian
25-3, 7	100	-18.7	30.0	0.6	$2.33E^{-5}$	4.1	
25-3, 92	100	26.2	257.2	0.3	$2.65E^{-5}$	9.2	
26-1, 45	100	-53.9	242.6	0.1	$7.54E^{-6}$	10.9	
26-1, 95	100	22.0	52.5	2.9	$4.40E^{-5}$	11.1	
26-1, 125	100	-9.3	120.0	0.4	$4.10E^{-5}$	8.8	
26-1, 145	100	-19.6	21.1	0.3	$1.05E^{-4}$	5.1	
26-2, 30	100	-7.2	260.2	0.2	$7.03E^{-5}$	3.7	Santonian
26-2, 55	100	19.7	334.4	0.0	$1.06E^{-4}$	11.8	
26-2, 79	100	-22.2	115.5	0.6	$4.17E^{-5}$	4.3	
26-2, 123	100	-23.6	360.0	1.4	$2.84E^{-5}$	12.8	
26-2, 143	100	-14.2	186.6	0.2	$2.19E^{-5}$	6.2	
Hole 317A							
5-1, 134	100	22.4	60.6	0.4	$1.08E^{-6}$	15.2	Lower Maestrichtian-upper Campanian
6-2, 30	100	-40.8	288.5	2.2	$1.36E^{-5}$	18.2	Middle Campanian
6-2, 32	100	-45.1	273.6	4.1	$1.44E^{-5}$	8.7	
6-2, 94	100	-50.0	142.2	0.4	$2.63E^{-5}$	10.8	
6-2, 96	100	-53.2	89.4	2.3	$2.51E^{-5}$	13.8	
7-1, 22	100	-27.2	75.9	1.8	$1.53E^{-5}$	7.4	Santonian
7-1, 24	100	-27.6	76.5	0.6	$1.90E^{-5}$	6.9	
7-1, 26	100	-48.3	76.3	0.9	$1.64E^{-5}$	9.1	
7-1, 144	100	-31.1	156.9	2.0	$2.16E^{-5}$	12.8	Lower Turonian-Cenomanian
81-, 115	100	-50.6	134.1	0.9	$8.23E^{-6}$	4.6	Cenomanian-upper Albian
8-1, 117	100	-51.7	131.2	1.2	$7.46E^{-6}$	3.6	
9-1, 44	100	-39.2	1.8	0.3	$5.95E^{-6}$	9.5	Lower-middle Albian
9-1, 46	100	-39.2	3.3	0.1	$5.51E^{-6}$	9.0	
9-1, 141	100	-41.3	265.6	0.2	$6.38E^{-6}$	5.2	
9-1, 143	100	-36.6	267.9	0.6	$5.85E^{-6}$	5.5	
9-1, 145	100	-39.0	267.3	0.3	$5.94E^{-6}$	2.9	
10-3, 24	100	-50.0	204.7	0.3	$2.54E^{-5}$	6.9	Upper Aptian and Aptian-Barremian
10-3, 132	100	-43.0	350.0	0.9	$1.59E^{-5}$	8.4	
11-2, 16	100	-58.6	326.2	1.3	$1.68E^{-5}$	4.7	
11-2, 18	100	-56.2	319.4	1.2	$1.81E^{-5}$	3.5	
11-2, 67	100	-45.5	224.8	0.1	$3.36E^{-5}$	5.2	
11-3, 45	100	-40.2	13.0	1.1	$2.14E^{-5}$	5.8	
11-3, 122	100	-45.0	259.9	0.4	$1.45E^{-5}$	3.3	
11-4, 141	100	-54.7	343.3	1.3	$8.33E^{-6}$	8.0	

TABLE 2 – *Continued*

Sample (Interval in cm)	Demagnetization Field	Incl. (degrees)	Decl. (degrees)	A (degrees)	Intensity (emu/cc)	MM (%)	F (Age)
11-5, 125	100	40.8	18.4	4.0	$6.02E^{-6}$	9.0	
13-1, 116	100	-58.1	265.2	0.5	$7.43E^{-5}$	10.0	
13-3, 67	100	-59.9	350.0	0.9	$4.75E^{-5}$	9.2	Upper Aptian
13-3, 144	100	-60.5	187.7	0.1	$1.58E^{-4}$	4.5	and
14-2, 29	100	-64.6	198.1	0.3	$1.14E^{-4}$	8.8	Aptian Barremian
14-3, 128	100	-60.4	276.9	1.2	$1.45E^{-4}$	6.3	
15-2, 17	100	-52.6	34.4	1.8	$1.19E^{-4}$	8.1	
15-4, 4	100	-61.6	70.5	0.3	$3.53E^{-4}$	11.1	
15-4, 6	100	-61.5	70.0	1.1	$2.59E^{-4}$	7.1	

plate motion (Sclater and Cox, 1970; Hammond et al., 1974) provided that the detrital remanent magnetization is acquired parallel to the earth's magnetic field and that secular variation is averaged out. Some coarse-grained sediments and varved sediments show an inclination error due to the effect of gravity or currents on the alignment of magnetic mineral grains during deposition. However, deep-sea sediments appear to have no inclination error (Opdyke and Henry, 1969; Jarrard, 1974), probably because the magnetization is a postdepositional remanent magnetization, resulting from rotation and alignment of magnetic mineral grains within the top few centimeters of sediment (Irving and Major, 1964; Kent, 1973). The few anisotropic susceptibility measurements on deep-sea sediments (Rees, 1971; Lovlie et al., 1973) indicate very low anisotropy and thus no inclination error.

Anisotropic susceptibility measurements were made on 47 samples from Holes 315A and 317A (Figure 6). The values of h (a measure of the magnitude of anistropy; Rees, 1974) for 315A samples range from 0.024 to 0.695 (x = 0.246, σ = 0.166) and for 317A samples from 0.097 to 0.323 (x = 0.196, σ = 0.044). These values of anisotropy are so small that probably little or no significant inclination error would result. Most previous anisotropic susceptibility measurements on unlithified deep-sea sediment cores (Harrison and Peterson, 1965; Lovlie et al., 1971) show vertical maximum susceptibility axes, in contrast to the horizontal maximum susceptibility axes commonly observed in sediments sampled on land and in lithified deep-sea sediments examined by Rees (1971). Maximum susceptibility axes on these lithified Leg 33 specimens are close to horizontal (Figure 6). Anisotropic susceptibility is sensitive to deformation. Possibly the commonly observed slight arching of unlithified sediments due to the coring process may account for the occurrence of vertical maximum susceptibility axes only in unlithified sediments.

Paleomagnetic evidence of Pacific plate motion since the Cretaceous is provided by magnetic surveys of seamounts (Francheteau et al., 1970; Harrison et al., in press), comparisen of magnetic anomaly amplitud on the two limbs of the Great Magnetic Bight (Vin, 1968), and model studies of magnetic anomalies of the Japanese, Hawaiian, and Phoenix lineations (Larson and Chase, 1972). These methods indicate about 30° of northward motion in the past 70-110 m.y., and possibly about 40° of northward motion in the past 135 m.y. Inclinations at DSDP Site 66 (at 2.4°N, 166.1°W) (Figure 1) are consistent with the above, indicating about 30° of northward motion of the Pacific plate since the Cretaceous (Sclater and Jarrard, 1971); however, the 95% confidence limits of these data are large (17.6°-46.9°). In contrast, DSDP Sites 166 and 167 (Figure 1) indicate significantly less northward motion of the Pacific plate, 18.9° (13.8°-31.6°) and 15.5° (13.8°-18.6°), respectively.

Median inclinations and 95% confidence limits of the median for each site, along with the resulting paleolatitudes, were calculated from reliable (A <5.0) 100-oe measurements and are summarized in Table 5 along with other paleolatitude data. Paleolatitudes (ϕ), based on the axial geocentric dipole assumption, were calculated using the formula: $\tan \phi = \frac{1}{2} \tan I$, where I is the median inclination for the site, Holes 315A and 317A sediment data indicate 13.3° (12.0-13.6°) and 18.7° (12.3-22.8°) northward motion for this area of the Pacific plate since the Late Cretaceous. These data in addition to Site 167 are tightly grouped and do not overlap with the seamount or magnetic anomaly data. One possible interpretation of these results is that the Pacific plate has been decoupled in this area at some time in the past.

A critical assumption in the determination of paleolatitudes from the inclination of remanent magnetization of basalts is that secular variation has been averaged out. Only 10 basalt flows were cored (Jackson et al., this volume) and sampled in Hole 317A, and only two thin layers of sediment were visible between flows. Thus, it is possible that the flows span only a short period of time and therefore that secular variation has not been averaged out. The small dispersion of remanance directions is consistent with this possibility. If the magnetic inclinations of Hole 317A basalts do provide a reliable indication of the axial geocentric dipole field, then the basalts were apparently formed at 48.3°S (43.7°-51.8°) indicating approximately 37° of northward motion (Table 5). The lowest sediment sample at this site (317A-15, 4-6 cm) is approximately 100 meters above the first basalt flow. The intervening 100 meters consist of volcanogenic sands (see Part I, this volume) which, in all probability, were deposited in a very short time period. The oldest recognizable fossil is

TABLE 3
Demagnetization of Basalt Pilot Samples

Sample (Interval in cm)	Demagnetization Field	Incl. (degrees)	Decl. (degrees)	*A* (degrees)	Intensity (emu/cc)	*MM* (%)
317A-31-2, 7	000	-56.4	322.3	0.4	$2.80E^{-3}$	2.1
	025	-62.5	314.2	0.4	$2.69E^{-3}$	2.1
	050	-67.0	305.4	0.5	$2.38E^{-3}$	2.7
	075	-68.0	298.0	0.3	$2.04E^{-3}$	1.8
	100	-68.3	299.8	0.5	$1.91E^{-3}$	2.0
	150	-68.3	298.0	0.4	$1.66E^{-3}$	1.9
	175	-68.8	293.7	0.4	$1.52E^{-3}$	1.9
	200	-69.0	294.8	0.2	$1.40E^{-3}$	2.1
	250	-69.0	293.0	0.3	$1.20E^{-3}$	2.4
	300	-68.7	293.7	0.3	$1.01E^{-3}$	3.0
	350	-68.0	287.8	1.1	$8.02E^{-3}$	3.4
	400	-67.2	293.9	0.3	$7.31E^{-4}$	4.1
	500	-70.5	292.8	0.2	$4.73E^{-4}$	8.9
317A-31-2, 7A	000	-64.5	318.6	0.1	$4.13E^{-3}$	3.7
	025	-66.3	313.7	0.2	$4.08E^{-3}$	3.5
	050	-66.6	310.5	0.1	$3.76E^{-3}$	3.0
	075	-67.2	309.5	0.2	$3.46E^{-3}$	2.5
	100	-66.7	308.3	0.1	$3.22E^{-3}$	3.3
	200	-66.8	304.9	0.2	$2.24E^{-3}$	3.2
	350	-66.3	303.9	0.2	$8.82E^{-4}$	3.9
	500	-67.5	303.0	0.5	$2.80E^{-4}$	4.3
317A-31-2, 37	000	-62.8	132.5	0.1	$3.79E^{-3}$	7.9
	025	-63.5	129.8	0.1	$3.73E^{-3}$	6.6
	050	-62.6	130.0	0.1	$3.42E^{-3}$	5.9
	075	-62.8	130.1	0.0	$3.10E^{-3}$	5.8
	100	-63.0	129.5	0.1	$2.91E^{-3}$	5.3
	150	-63.0	128.1	0.1	$2.55E^{-3}$	5.3
	200	-63.0	127.3	0.2	$2.17E^{-3}$	4.9
	300	-63.3	126.6	0.2	$1.46E^{-3}$	5.0
	500	-63.4	126.2	0.3	$5.93E^{-4}$	5.7
317A-31-4, 43A	000	-65.1	91.8	0.5	$4.49E^{-3}$	17.5
	025	-64.9	92.0	0.1	$3.98E^{-3}$	6.6
	050	-66.7	85.5	0.3	$3.61E^{-3}$	4.1
	075	-67.4	81.4	0.2	$3.29E^{-3}$	3.9
	100	-67.4	80.0	0.5	$3.10E^{-3}$	3.2
	150	-68.0	76.0	0.5	$2.72E^{-3}$	3.4
	200	-68.1	74.8	0.5	$2.31E^{-3}$	3.4
	250	-68.1	73.7	0.4	$1.95E^{-3}$	3.1
	300	-68.0	70.4	0.1	$1.56E^{-3}$	1.7
	350	-67.4	71.5	0.5	$1.23E^{-3}$	2.9
	400	-68.0	72.8	0.5	$9.39E^{-4}$	3.5
	500	-67.2	74.9	0.7	$5.24E^{-4}$	3.6
317A-32-4, 77	000	-77.8	286.7	0.1	$4.52E^{-3}$	3.7
	025	-80.2	290.2	0.1	$4.43E^{-3}$	6.0
	050	-77.3	292.9	0.1	$4.22E^{-3}$	4.7
	075	-72.7	286.8	0.0	$4.09E^{-3}$	1.8
	100	-72.0	286.7	0.0	$3.94E^{-3}$	2.2
	150	-70.6	285.9	0.0	$3.53E^{-3}$	2.0
	200	-65.2	302.1	4.0	$2.52E^{-3}$	21.3
	250	-68.2	284.9	0.1	$2.40E^{-3}$	1.2
	300	-70.1	284.6	0.1	$2.11E^{-3}$	1.6
	400	-70.5	283.6	0.2	$1.40E^{-3}$	1.9
	500	-70.4	284.7	0.0	$9.19E^{-4}$	1.3
	560	-70.2	282.9	0.0	$6.99E^{-4}$	1.5
	630	-70.7	282.9	0.2	$5.36E^{-4}$	1.9
	750	-71.0	286.2	1.0	$3.54E^{-4}$	10.4
	800	-70.9	284.4	0.1	$3.00E^{-4}$	3.6

TABLE 3 – *Continued*

Sample (Interval in cm)	Demagnetization Field	Incl. (degrees)	Decl. (degrees)	*A* (degrees)	Intensity (emu/cc)	*MM* (%)
	850	-62.1	279.9	0.7	$2.23E^{-4}$	22.0
	950	-66.4	303.6	1.8	$2.15E^{-4}$	7.9
317A-32-5, 79A	000	-72.7	261.8	0.1	$2.47E^{-3}$	1.3
	010	-88.6	201.9	0.6	$2.46E^{-3}$	17.0
	025	-72.1	263.1	0.2	$2.41E^{-3}$	1.4
	050	-72.2	262.4	0.3	$2.25E^{-3}$	1.4
	075	-71.5	258.4	0.1	$2.06E^{-3}$	1.1
	100	-71.0	258.9	0.3	$1.91E^{-3}$	1.2
	150	-70.7	255.5	0.2	$1.61E^{-3}$	0.5
	200	-70.5	253.2	0.2	$1.34E^{-3}$	1.7
	300	-70.0	250.0	0.3	$8.52E^{-4}$	1.5
	400	-68.5	250.2	0.1	$4.89E^{-4}$	1.3
	700	-68.1	242.6	0.4	$8.68E^{-5}$	3.1
317A-34-4, 125B	000	-62.9	234.8	0.1	$6.15E^{-3}$	1.9
	025	-63.0	233.0	0.1	$6.08E^{-3}$	1.5
	050	-62.4	233.2	0.1	$5.95E^{-3}$	1.4
	100	-62.0	231.8	0.0	$5.63E^{-3}$	1.4
	200	-62.2	231.1	0.2	$4.65E^{-3}$	1.9
	300	-61.9	231.7	0.1	$3.20E^{-3}$	2.1
	500	-61.5	231.1	0.1	$1.31E^{-3}$	2.2
	700	-61.7	230.7	0.2	$6.09E^{-4}$	1.9
	900	-61.8	230.2	0.1	$3.52E^{-4}$	1.5

found in Core 13 (see Part I, this volume), approximately 20 meters above our lowest sample, and is given an age of about 107 m.y. (see Part I, this volume). A minimum K-Ar age for the basalt is 106 ±3.5 m.y. (Lanphere and Dalrymple, this volume) which is concordant with the sediment age. It seems unlikely that the basalts were formed 20° farther south than the sediments. Two alternative explanations are (1) secular variation has not been averaged out, or (2) tectonic tilting of the basalt occurred either prior to or contemporaneously with volcanogenic sedimentation. If these basalts were formed at an ancient spreading center, then they would be subject to the slight tilting commonly associated with tectonic activity at mid-ocean ridges. However, the few flow contacts in these basalt cores are close to horizontal, which seems inconsistent with the hypothesis of substantial tilting. A third possibility is that remanent inclinations of the sediments have been modified during compaction. Though remanent inclinations of Deep Sea Drilling sediments from the Wharton Basin (Jarrard, 1974) showed no evidence of compaction errors, further studies are underway to evaluate this possibility.

MAGNETIC REVERSALS

The Cretaceous reversal pattern is dominated by a long interval of almost exclusively normal polarity (Helsley and Steiner, 1969), extending from the Barremian to about the Campanian-Maestrichtian boundary (Keating et al., 1975; Jarrard and Tovish, in preparation). The estimated ages of basalt in Holes 315A and 317A are about 85 m.y. and 110 m.y., respectively, both well within this normal interval. Thus the occurrence of exclusively normal polarity in the basalt samples from Holes 315A and 317A is not surprising.

Most samples of sediment from Holes 315A and 317A are of normal polarity. Several single specimens from both sites have positive inclinations and thus may be reversely polarized, but further sampling is needed to confirm these possible reversals. One definitely reversed interval has been detected: in Hole 315A between Core 15, Section 1, and Core 18, Section 3, perhaps split by a short normal interval (Table 2). These sediments, upper Paleocene to middle Maestrichtian in age, are from the Tertiary and Maestrichtian mixed polarity interval (Heirtzler et al., 1968; Sclater et al., 1973) which followed the Cretaceous long interval of dominantly normal polarity. Cores 19 to 27 in Hole 315A and all paleomagnetically sampled cores from Hole 317A are paleontologically dated as within the Campanian to Barremian interval and consequently are almost exclusively of normal polarity.

ACKNOWLEDGMENTS

We thank B.P. Luyendyk for discussions throughout this project and for reviewing the manuscript. This research was supported by National Science Foundation Grants GA-36589 and DES75-03709.

REFERENCES

Doell, R.R. and Cox. A., 1965. Measurement of the remanent magnetization of igneous rocks: U.S. Geol. Surv. Bull. 1203-A, p. 1-32.

Francheteau, J., Harrison, C.G.A., Sclater, J.G., and Richards, M.L., 1970. Magnetization of Pacific seamounts: a preliminary polar curve for the northeastern Pacific: J. Geophys. Res., v. 75, p. 2035-2061.

Hammond, S.R., Theyer, F., and Sutton, G.H., 1974. Paleomagnetic evidence of northward movement of the Pacific plate in deep-sea cores from the central Pacific Basin: Earth Planet. Sci. Lett., v. 22, p. 22-28.

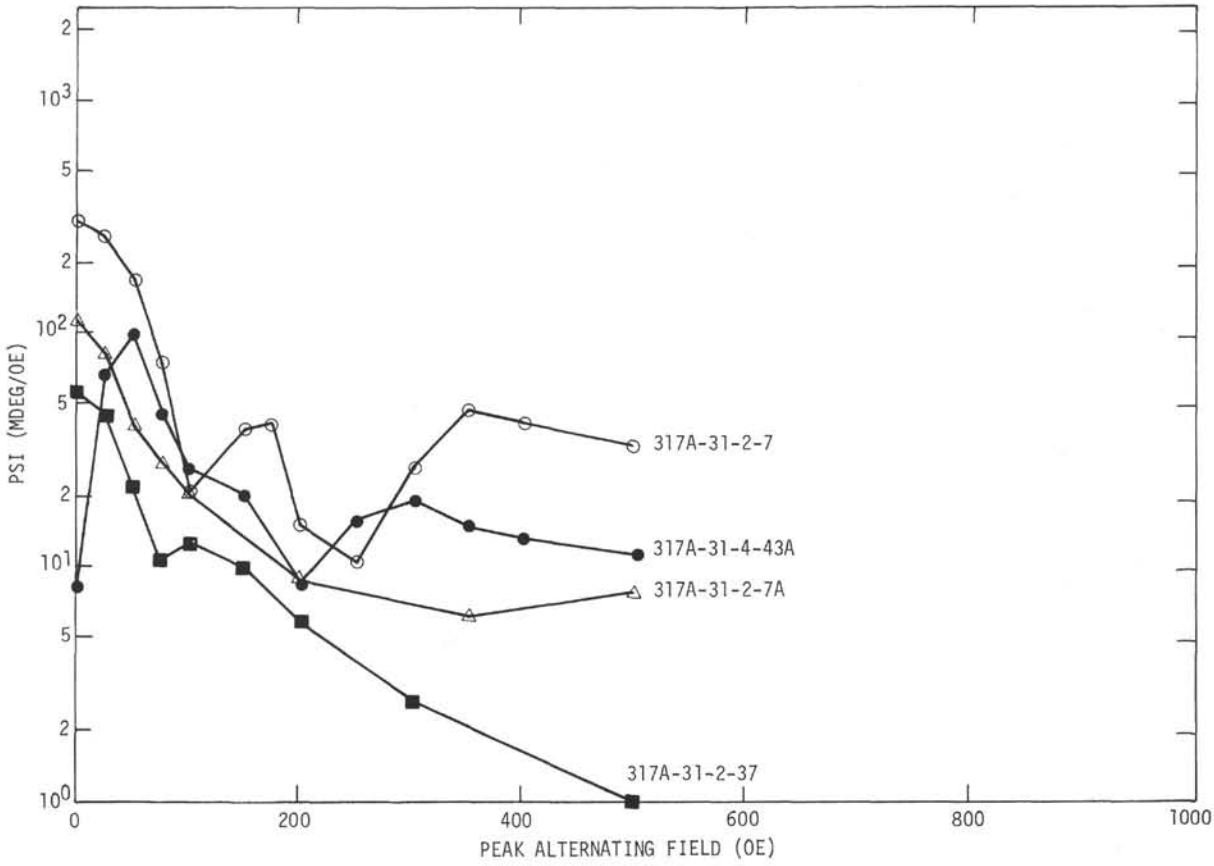

Figure 4. *Log PSI demagnetization curves for DSDP Hole 317A basalts. See text for discussion of PSI.*

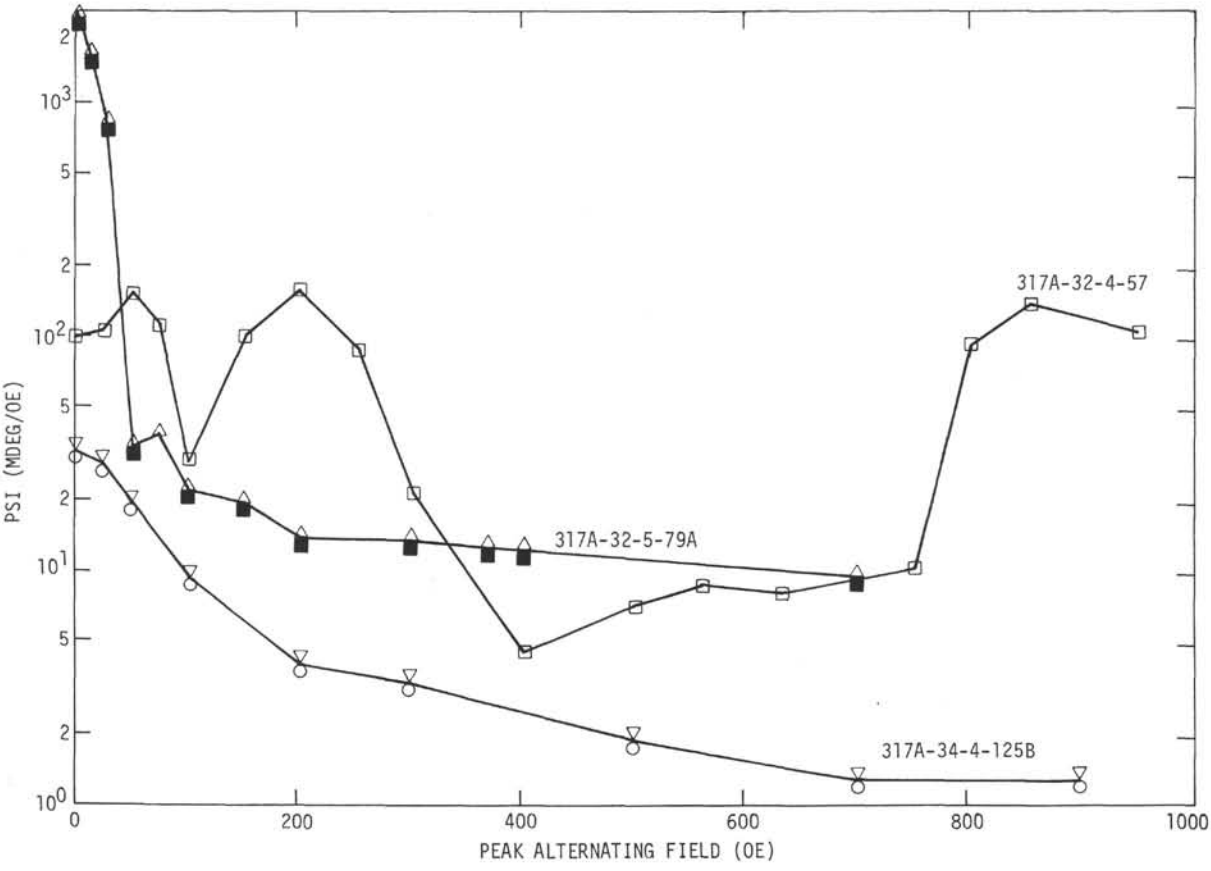

Figure 4. *(Continued).*

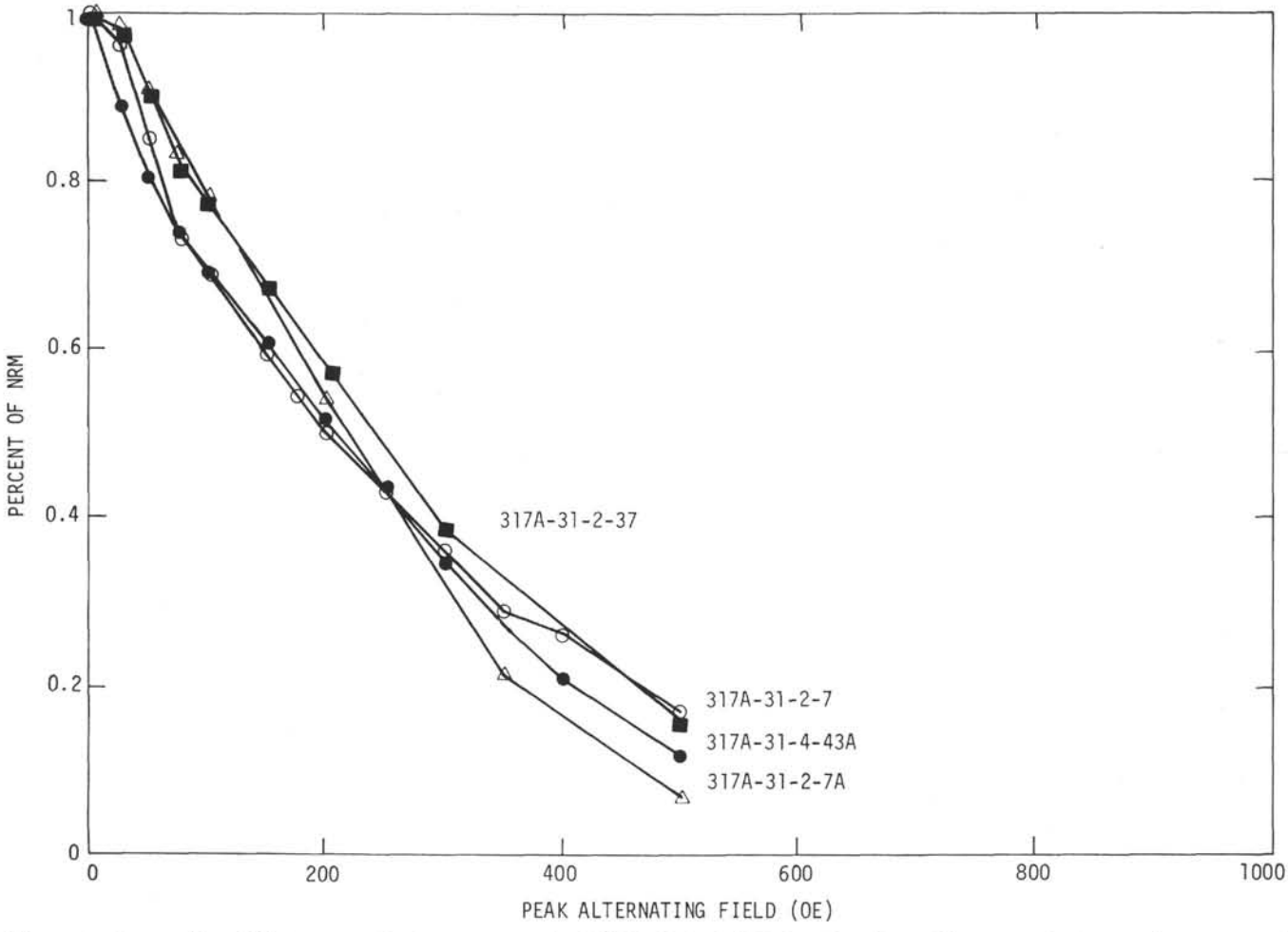

Figure 5. *Progressive AF demagnetization curves for DSDP Hole 317A basalts. Intensities are relative to the untreated (NRM) values.*

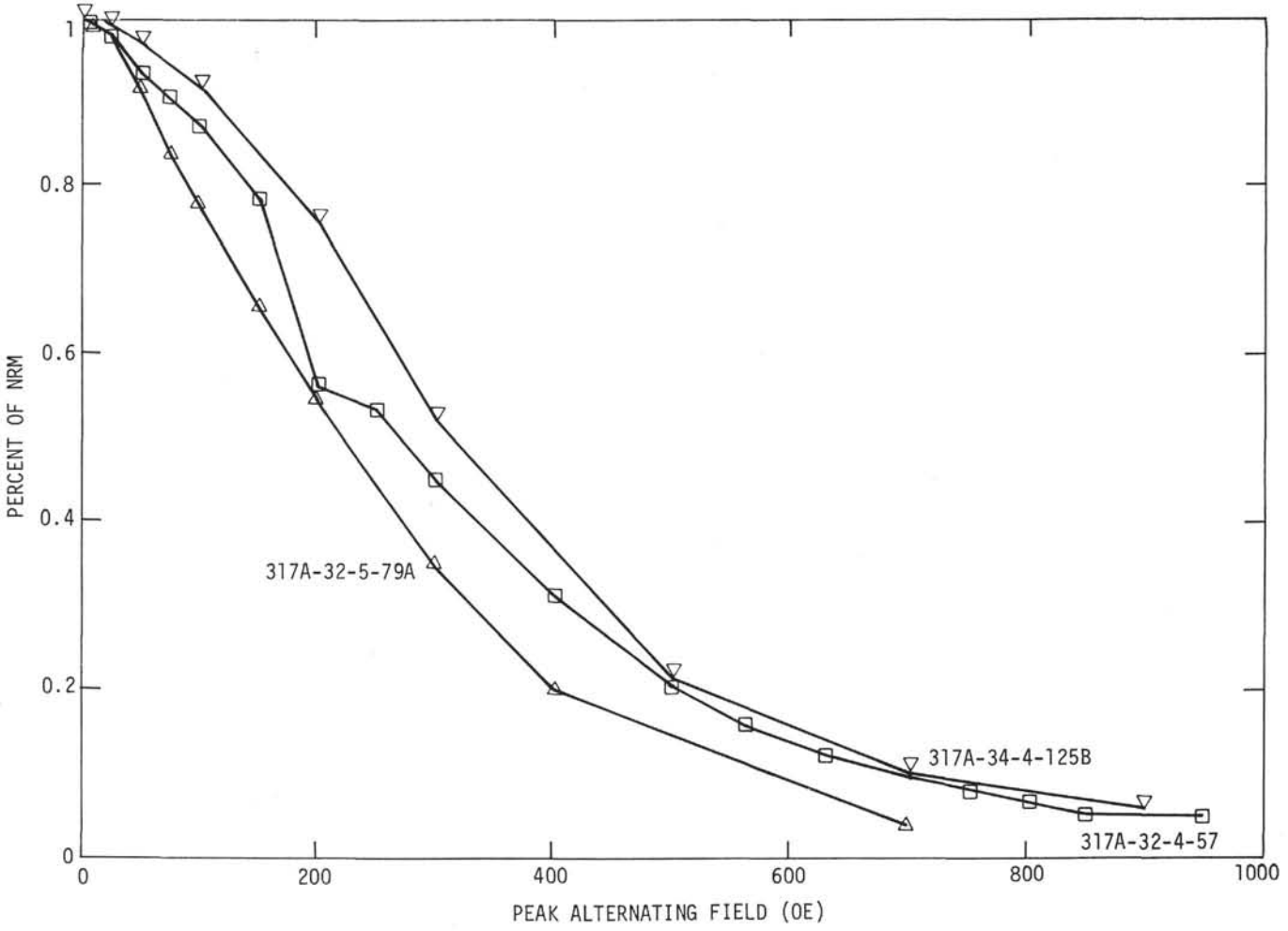

Figure 5. *(Continued).*

TABLE 4
Results of Paleomagnetic Measurements of Hole 317A Basalts

Sample (Interval in cm)	NRM					250 oe					
	Incl.	Decl.	*A*	Intensity (emu/cc)	*MM* (%)	Incl.	Decl.	*A*	Intensity (emu/cc)	*MM* (%)	FN[a]
31-2, 7	-56.4	322.3	0.4	$2.80E^{-3}$	2.1	-69.0	293.0	0.3	$1.20E^{-3}$	2.4	1
31-2, 7A[b]	-64.5	318.6	0.1	$4.13E^{-3}$	3.7	-66.8	304.9	0.2	$2.24E^{-3}$	3.2	
31-2, 37[b]	-62.8	132.5	0.1	$3.79E^{-3}$	7.9	-63.0	127.3	0.2	$2.17E^{-3}$	4.9	2
31-2, 75						-67.2	181.7	0.0	$2.82E^{-3}$	4.6	
31-3, 12						-65.6	166.8	0.8	$5.39E^{-4}$	3.1	3
31-3, 102						-77.6	233.1	0.1	$1.23E^{-3}$	9.0	4
31-4, 43A	-65.1	91.8	0.5	$4.49E^{-3}$	17.5	-68.1	73.7	0.4	$1.95E^{-3}$	3.1	
31-4, 43B						-66.7	76.6	0.1	$1.89E^{-3}$	2.9	
31-4, 127A	-73.7	41.1	0.4	$4.38E^{-3}$	3.8	-71.9	26.5	0.1	$2.32E^{-3}$	1.6	
31-4, 127B	-70.5	30.6	0.0	$4.13E^{-3}$	1.9	-71.8	24.8	0.2	$2.35E^{-3}$	2.7	
32-1, 57A	-60.2	160.1	0.5	$4.76E^{-3}$	12.9	-59.3	152.1	0.1	$2.53E^{-3}$	7.8	
32-1, 57B	-62.1	161.3	0.1	$5.33E^{-3}$	21.4	-61.9	154.8	0.5	$2.82E^{-3}$	4.3	
32-1, 132B	-71.9	58.0	0.2	$3.95E^{-3}$	4.2	-71.0	52.4	0.5	$2.29E^{-3}$	1.1	5
32-1, 132C	-70.2	57.6	0.1	$4.16E^{-3}$	4.1	-67.3	54.1	0.3	$2.77E^{-3}$	5.3	
32-2, 130A	-70.8	56.8	0.1	$4.01E^{-3}$	2.4	-69.2	48.4	0.2	$2.15E^{-3}$	2.3	
32-2, 130B	-72.5	61.7	0.3	$3.73E^{-3}$	6.3	-69.0	47.3	0.1	$1.85E^{-3}$	3.6	
32-3, 74	-69.5	226.3	0.2	$4.25E^{-3}$	4.2	-68.9	222.9	0.3	$2.14E^{-3}$	3.1	
32-4, 55A	-64.3	71.9	0.6	$5.28E^{-3}$	1.6	-69.0	63.6	0.3	$2.21E^{-3}$	0.7	
32-4, 55B	-70.1	60.6	0.5	$4.68E^{-3}$	4.1	-68.3	56.1	0.3	$2.17E^{-3}$	4.4	
32-4, 77[c]	-77.8	286.7	0.1	$4.52E^{-3}$	3.7	-68.2	284.9	0.1	$2.40E^{-3}$	1.2	
32-4, 101A	-72.8	260.7	0.4	$3.04E^{-3}$	1.6	-63.3	253.0	0.3	$1.61E^{-3}$	2.6	
32-4, 101C	-71.5	250.6	0.1	$3.27E^{-3}$	2.1	-70.6	239.0	0.9	$1.48E^{-3}$	5.3	
32-5, 79A[b]	-72.7	261.8	0.1	$2.47E^{-3}$	1.3	-70.5	253.2	0.2	$1.34E^{-3}$	1.7	
32-5, 79B	-70.8	262.6	0.2	$2.73E^{-3}$	1.7	-61.0	251.4	0.2	$1.16E^{-3}$	1.8	6
32-5, 79C	-67.7	260.5	0.9	$2.65E^{-3}$	5.1	-59.8	251.3	0.2	$1.14E^{-3}$	4.1	
32-6, 128A	-71.4	194.4	0.9	$1.86E^{-3}$	15.5	-52.5	134.2	0.3	$2.66E^{-4}$	3.9	
33-3 100	-66.5	247.1	0.1	$2.54E^{-3}$	1.0	-68.5	248.4	0.1	$1.38E^{-3}$	2.1	
33-4, 62	-56.3	116.4	0.1	$7.29E^{-3}$	2.6	-55.3	117.6	0.1	$3.64E^{-3}$	1.5	
34-1, 70A	-73.8	338.9	0.1	$8.38E^{-3}$	2.0	-69.3	336.1	0.1	$3.24E^{-3}$	1.7	7
34-1, 70B	-70.8	348.0	0.2	$7.88E^{-3}$	3.9	-69.4	341.4	0.1	$3.28E^{-3}$	2.7	
34-2, 31	-67.4	45.3	0.2	$8.23E^{-3}$	3.9	-66.9	46.0	0.2	$4.54E^{-3}$	3.9	8
34-2, 128.5A	-67.5	229.2	0.1	$2.64E^{-3}$	4.2	-62.7	220.3	0.3	$5.12E^{-4}$	4.3	9
34-2, 128.5B	-65.9	235.2	0.4	$2.85E^{-3}$	2.9	-62.0	222.2	0.4	$5.13E^{-4}$	3.7	
34-3, 50A	-42.5	173.6	0.5	$5.44E^{-3}$	4.0	-41.6	172.2	0.9	$2.46E^{-3}$	4.9	
34-3, 50B	-44.2	176.4	0.1	$5.56E^{-3}$	3.7	-49.5	171.7	0.2	$3.09E^{-3}$	5.9	
34-4, 125B[b]	-62.9	234.8	0.1	$6.15E^{-3}$	1.9	-62.2	231.1	0.2	$4.65E^{-3}$	1.9	10
34-4, 125C	-62.3	232.4	0.2	$7.50E^{-3}$	3.5	-57.6	235.6	0.8	$4.55E^{-3}$	3.7	
34-4, 125D	-64.8	231.3	0.3	$7.23E^{-3}$	2.4	-62.7	228.4	0.3	$4.30E^{-3}$	2.1	

[a]Flow numbers (FN) from Jackson et al., this volume.

[b]AF demagnetization at 200 oe.

[c]AF demagnetization at 300 oe.

Harrison, C.G.A. and Peterson, M.N.A., 1965. A magnetic mineral from the Indian Ocean: Am. Mineral., v. 50, p. 704-712.

Harrison, C.G.A., Jarrard, R.D., Vacquier, V., and Larson, R.L., in press. Palaeomagnetism of Cretaceous Pacific seamounts: Geophys. J.

Heirtzler, J., Dickson, G.O., Herron, E.M., Pitman, W.C., III, and LePichon, X., 1968. Marine magnetic anomalies, geomagnetic field reversals, and motions of the ocean floor and continents: J. Geophys. Res., v. 73, p. 2119-2136.

Helsley, C.E. and Steiner, M.B., 1969. Evidence for long intervals of normal polarity during the Cretaceous period: Earth Planet. Sci. Lett., v. 5, p. 325-332.

Irving, E. and Major, A., 1964. Post-depositional remanent magnetization in a synthetic sediment: Sedimentology, v. 3, p. 135-143.

Jarrard, R.D., 1973. Paleomagnetism of Leg 17 sediment cores. *In* Winterer, E.L., Ewing, J.L., et al., Initial Reports of the Deep Sea Drilling Project, Volume 17: Washington (U.S. Government Printing Office), p. 365-376.

_____, 1974. Paleomagnetism of some Leg 27 sediment cores. *In* Veevers, J.J. Heirtzler, J.R., et al., Initial Reports of the Deep Sea Drilling Project, Volume 27: Washington (U.S. Government Printing Office), p. 415-423.

Jarrard, R.D. and Tovich, A., in preparation. Cretaceous reversal chronology.

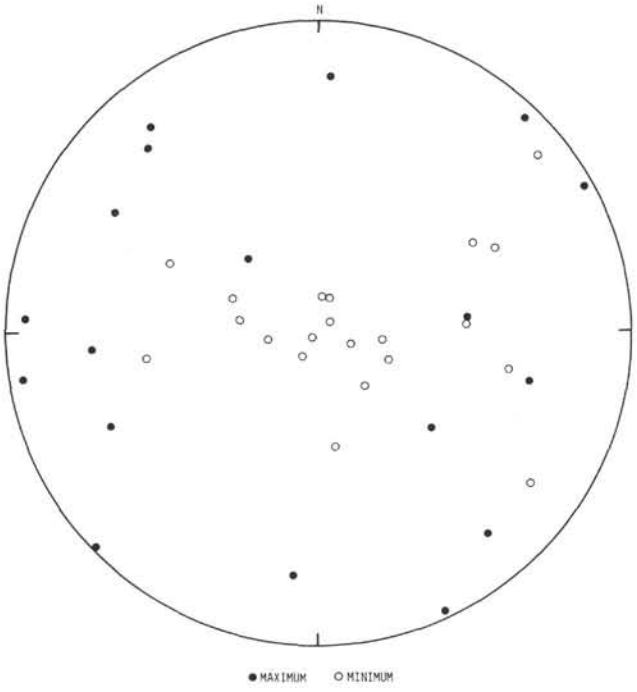

Figure 6a. *Lower hemisphere stereograms showing the directions of minimum and maximum anisotropy of susceptibility axes in Hole 315A samples. N is the pole relative to the split face of the core, but has no geographical significance.*

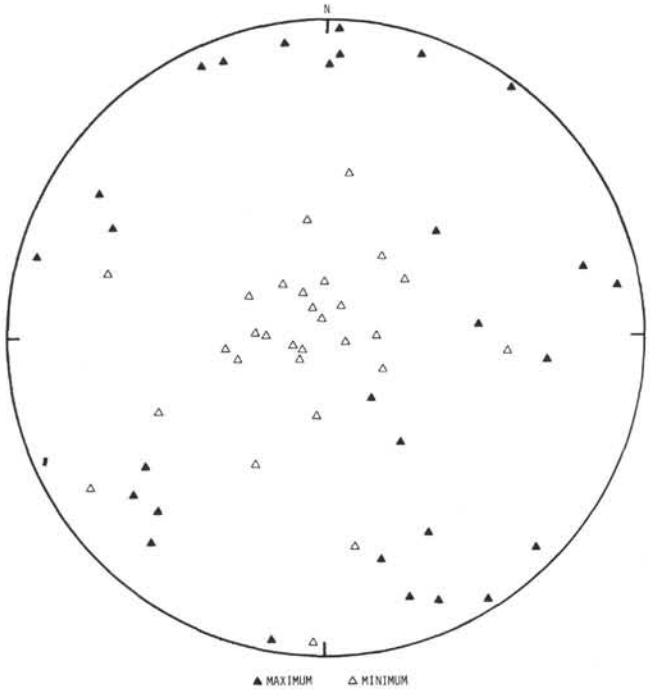

Figure 6b. *Lower hemisphere stereograms showing the directions of minimum and maximum anisotropy of susceptibility axes in Hole 317A samples. N is the pole relative to the split face of the core, but has no geographical significance.*

Keating, B., Helsley, C.E., and Passagno, E.A., Jr., 1975. Late Cretaceous reversal sequence: Geology, v. 3, p. 73-76.

Kent, D., 1973. Post-depositional remanent magnetization in deep-sea sediment: Nature, v. 256, p. 32-34.

Larson, R.L. and Chase, C.G., 1972. Late Mesozoic evolution of the western Pacific Ocean: Geol. Soc. Am. Bull., v. 83, p. 3627-2644.

Lovlie, R., Lowrie, W., and Jacobs, M., 1971. Magnetic properties and mineralogy of four deep-sea cores: Earth Planet. Sci. Lett., v. 15, p. 157-168.

Lowrie, W., Lovlie, R., and Opdyke, N.D., 1973a. Magnetic properties of Deep Sea Drilling Project basalts from the north Pacific Ocean: J. Geophys. Res., v. 78, p. 7647-7660.

———, 1973b. The magnetic properties of Deep Sea Drilling Project basalts from the Atlantic Ocean: Earth Planet. Sci. Lett., v. 17, p. 338-349.

Marshall, M., in preparation. The magnetic properties of some DSDP basalts from the north Pacific and Pacific plate tectonics.

Opdyke, N.D. and Henry, D.W., 1969. A test of the dipole hypothesis: Earth Planet. Sci. Lett., v. 6, p. 139-151.

Park, J.K. and Irving, E., 1970. The mid-Atlantic Ridge near 45°N. XII. Coercivity, secondary magnetization, polarity, and thermal stability of dredge samples: Canadian J. Earth Sci., v. 7., p. 1499-1514.

Peirce, J.W., Denham, C.R., and Luyendyk, B.P., 1975. Paleomagnetic results of basalt samples from DSDP Leg 26, southern Indian Ocean. *In* Davies, T.A., Luyendyk, B.P., et al., Initial Reports of the Deep Sea Drilling Project, Volume 26: Washington (U.S. Government Printing Office), p. 517-527.

Rees, A.I., 1964. Measurements of the natural remanent magnetism and anisotropy of susceptibility of some Swedish glacial silts: Geophys. J., v. 8, p. 356-369.

———, 1971. The magnetic anisotropy of samples from the Deep Sea Drilling Project Leg 1, Orange Texas to Hoboken, N.J.: Marine Geol., v. 11, p. M16-M23.

Sclater, J.G and Cox, A., 1970. Palaeolatitudes from JOIDES deep sea sediment cores: Nature, v. 226, p. 934-935.

Sclater, J.G. and Jarrard, R.D., 1971. Preliminary paleomagnetic results, Leg 7. *In* Winterer, E.L., Riedel, W.R., et al., Initial Reports of the Deep Sea Drilling Project, Volume 7: Washington (U.S. Government Printing Office), p. 1227-1234.

Sclater, J.G., Jarrard, R.D., McGowran, B., and Gartner, S., Jr., 1974. Comparison of the magnetic and biostratigraphic time scales since the Late Cretaceous. *In* van der Borch, C.C., Sclater, J.G., et al., Initial Reports of the Deep Sea Drilling Project, Volume 22: Washington (U.S. Government Printing Office), p. 381-386.

Symons, D.T.A. and Stupavaky, M., 1974. A rational paleomagentic stability index: J. Geophys. Res., v. 79, p. 1718-1720.

Vine, F.J., 1968. Paleomagnetic evidence for the northward movement of the north Pacific Basin during the past 100 m.y. (abstract): Am. Geophys. Union Trans., v. 49, p. 156.

TABLE 5
Paleolatitudes from Core Inclinations

DSDP Site	Number of Samples	Median Inclination	95% Confidence Limits	Present Latitude	Paleolatitude	95% Confidence Limits	Amounts of Northward Motion	95% Confidence Limits	Age of Sampled Interval
66[a]	32	47.8°	28.8-63.2	2.5°N	28.9	15.4-44.7	31.1°	17.6-46.9	Senonian
166[b]	45	28.5°	19.5-46.6	3.7°N	15.2	10.1-27.9	18.9°	13.8-31.6	Late Eocene to late Hauterivian
167[b]	47	16.7°	13.8-22.3	7.0°N	8.5	6.8-11.6	15.5°	13.8-18.6	Late Campanian to late Albian-early Cenomanian
315A	82	17.8°	15.3-19.4	4.2°N	9.1	7.8-9.4	13.3°	12.0-13.6	Upper Paleocene to Santonian
317A (sediments)	33	48.3°	40.8-53.2	11.0°S	29.7	23.3-33.8	18.7°	12.3-22.8	Lower Maestrichtian-upper Campanian to Barremian-Aptian
317A (basalts)	10	65.4°	62.3-67.9	11.0°S	47.5	43.6-50.9	36.5°	32.6-39.9	106 ±3.5 m.y.
Seamounts[d]	26						31.7°	$\alpha 95 = 4.8$	85–110 m.y.

[a]Sclater and Jarrard, 1971.

[b]Jarrard, 1973.

[c]Harrison et al., in press.